Application of a coupled microwave, energy and water transfer model to relate passive microwave emission from bare soils to near-surface water content and evaporation

L. P. Simmonds, E. J. Burke

Hydrology and Earth System Sciences, 3(1), *31–38* (1999) © EGS

Hydrology & Earth System Sciences

Application of a coupled microwave, energy and water transfer model to relate passive microwave emission from bare soils to near-surface water content and evaporation

L.P. Simmonds[1] and E.J. Burke[2]

[1] Department of Soil Science, The University of Reading, Whiteknights, Reading RG6 6DW
[2] Institute of Hydrology, Crowmarsh Gifford, Wallingford, Oxon OX10 8BB, UK

Abstract

The paper examines the stability of the relation between microwave emission from the soil and the average near-surface water content in the case of relatively smooth, bare soils, and then considers the extent to which microwave radiometry can be used to estimate the effective surface resistance to vapour transfer, which is also related to the near-surface water status. The analysis is based on the use of a model (MICRO-SWEAT) which couples a microwave radiative transfer model with a SVAT scheme that describes the exchanges of water vapour, energy and sensible heat at the land surface. Verification of MICRO-SWEAT showed good agreement (about 3K RMSE) between predicted L band (1.4 GHz) brightness temperature over soils with contrasting texture during a multi-day drydown, and those measured using a truck-mounted radiometer. There was good agreement between the measured and predicted relations between the average water content of the upper 2 cm of the soil profile and the brightness temperature normalised with respect to the radiometric surface temperature. Some of the scatter in this relationship was attributable to diurnal variation in the magnitude of near-surface gradients in temperature and water content, and could be accounted for by using the physically-based simulation model. The influence of soil texture on this relationship was well-simulated using MICRO-SWEAT. The paper concludes by demonstrating how MICRO-SWEAT can be used to establish a relationship between the normalised brightness temperature and the surface resistance for use in the prediction of evaporation using the Penman-Monteith equation.

Introduction

There has been much research into the use of passive microwave radiometry for remotely sensing the average water content of the upper few centimetres of the soil profile (Schmugge *et al.*, 1986; Jackson and Schmugge, 1989; Schmugge and Jackson, 1994). Other work, motivated by the possibilities for inferring near-surface water content from remote sensing, has attempted to link evaporation rates to near surface water content (Mahfouf and Noilhan, 1991; Daamen and Simmonds, 1996). This paper attempts to integrate these two lines of research, and is based on recent work developing a model (MICRO-SWEAT) which couples a microwave radiative transfer model with a SVAT scheme that describes the exchanges of water vapour, energy and sensible heat at the land surface (Burke, 1997; Burke *et al.*, 1997a&b). Approaches to relate bare soil evaporation to the remote sensing of surface temperature and wetness using thermal and microwave radiometry (Camillo and Gurney, 1986; Bruckler and Witono, 1989; Chanzy *et al.*, 1995) have generally been based on relationships between average near-surface water content and evaporation (either via soil surface resistance, surface humidity or the actual:potential evaporation ratio) that depend strongly on the soil water retention and conductivity characteristics.

Materials and methods

MICRO-SWEAT

The model (MICRO-SWEAT) has two components. SWEAT, an established model of simultaneous water and heat transfer in the soil-vegetation-atmosphere system (Daamen and Simmonds, 1996) is used to predict the courses of the profiles of soil temperature and soil water content. These outputs are then passed into a microwave transfer model to predict the emission and fluxes of microwave radiation between soil layers, culminating in the prediction of the microwave flux emergent at the soil surface, which can be compared with the emission measured by radiometers mounted above the soil surface.

SWEAT is based on solution of the Richards' equation

to describe water flow through soils, and uses the following functions to describe the water retention and conductivity characteristics of the soil layers:

$$\theta = \theta_{sat}\left(\frac{\psi_e}{\psi}\right)^{-\frac{1}{b}} \quad \text{and} \quad K = K_{sat}\left(\frac{\psi_e}{\psi}\right)^{2+3/b} \qquad (1)$$

where θ is the volumetric water content, ψ and ψ_e are the matric and air entry potentials, K and K_{sat} are the unsaturated and saturated hydraulic conductivity, b is a 'shape' parameter, and θ_{sat} is the saturated water content, estimated from the bulk density.

In the case of bare soil, water and heat fluxes in the soil are coupled to the aerial environment using the principles of the Penman-Monteith equation, with the surface resistance term eliminated through knowledge of the humidity in the surface soil layer. The energy input through net radiation was either measured directly or modelled.The relevant outputs of SWEAT are the predictions of soil temperatures and water contents, which provided inputs to the microwave model.

The microwave component of the model is as follows. The flux emergent at the soil surface, expressed in terms of the equivalent microwave brightness temperature (T_B), is calculated as:

$$T_B = \Sigma f_i T_i + r_{surf} T_{sky} \qquad (2)$$

where the T_i are the soil temperatures in each soil layer (predicted using SWEAT), r_{surf} (= 1 – emissivity of the surface layer) is the surface reflectance and T_{sky} is the radiometric temperature of the sky. The fractional contribution of each soil layer (f_i) to the microwave flux emergent at the soil surface depends on the emissivity of each layer, and is simulated using the Wilheit (1978) model. The Wilheit model uses knowledge of the dielectric and temperature of each layer to predict the emission from each layer, and takes account of the attenuation of the electromagnetic flux as it flows through the soil in response to the electric field. The dielectric for each soil layer is related to the soil water content using the semi-empirical mixing model of Wang and Schmugge (1980), in which the overall dielectric of the layer depends on the contributions from the soil solids, bound water and free water present. The partitioning of water content between bound and free water is based empirically on the soil particle size distribution, with clay soils having greater bound water content.

The effective temperature of the soil with respect to the emission of microwave radiation (T_{eff}) is given by:

$$T_{eff} = \frac{\Sigma T_i f_i}{\Sigma f_i} \qquad (3)$$

and the average depth of origin of radiation emitted at the soil surface is given by the thermal sampling depth, z_t:

$$z_t = \frac{\Sigma z_i f_i}{\Sigma f_i} \qquad (4)$$

THE EXPERIMENTS

The paper is based mainly on the analysis of data obtained during an experiment in 1985, carried out at the USDA Beltsville Agricultural Research Center, Maryland, USA. Microwave brightness temperatures were monitored at a number of times each day throughout a succession of drydown periods following 100 mm irrigations of the experimental plots. The plots concerned in this paper were unvegetated, and provided a contrast in soil texture. The 10 m × 10 m plots had raised borders which contained either the native soil (a loamy sand; 75% sand, 5% clay) or an imported soil (a loam; 45% sand, 22% clay) with a depth of 25 cm overlying the native soil. Half-hourly records of net radiation, wet and dry bulb temperature, air temperatures and windspeed were available from an automatic weather station, thereby providing the atmospheric variables to drive the SWEAT component of MICRO-SWEAT. A dual polarised L band (21 cm wavelength, 1.4 GHz) passive microwave radiometer was used to monitor the microwave brightness temperature on three occasions each day during a number of multi-day drydowns following irrigation of the plots. Simultaneous measurements of radiometric surface temperature were made using a thermal infrared thermometer (8–14 μm, accuracy ± 0.5K), assuming an emissivity of 0.98. The radiometers were mounted on an 8 m truck boom (mounted 10° off nadir), at a nominal height of 6 m above the soil surface. The footprint of the microwave radiometer was approximately 1.5 m. At the same time that microwave brightness temperatures were measured, three replicate samples of soil (0–2 cm depth) were taken from just outside the field of view of the radiometer for the determination of water content by oven drying, which was converted into a volumetric soil water content from knowledge of the bulk density. Several other measurements made during the course of the experiment are not relevant to the analysis presented here, and are discussed elsewhere (Burke, 1997).

Results

Figure 1 illustrates the success with which MICRO-SWEAT predicts the diurnal courses of microwave brightness temperature (T_B) during a multi-day drydown following a large irrigation. The example is taken from one of the drydowns in the 1985 experiment in which detailed diurnal measurements were made of T_B over the bare surfaces of the two soils. The parameterization of MICRO-SWEAT used to produce the simulated time courses in Fig. 1 was based on half-hourly measurements of net radiation, humidity, air temperature and windspeed obtained from an automatic weather station. The water retention and hydraulic conductivity characteristics of the soils used in the simulations were obtained by an optimisation procedure to minimise the root mean square error between the measured and predicted microwave brightness temperatures. However, the soil hydraulic parameters derived in

this way were very close to those determined by direct measurement (Burke *et al.*, 1997b). The model predicted the course of brightness temperature with a root mean square error between the predicted and measured temperatures of about 3 K, which is of similar magnitude to the measurement error of the radiometer. The main features to note in Fig. 1 are the dramatic reduction in emissivity immediately following irrigation, after which emissivity increased from day to day as the surface dried. Superimposed on the day-to-day trend was a diurnal oscillation in brightness temperature which is attributable to the diurnal temperature fluctuation and also to the diurnal variation in near surface water status.

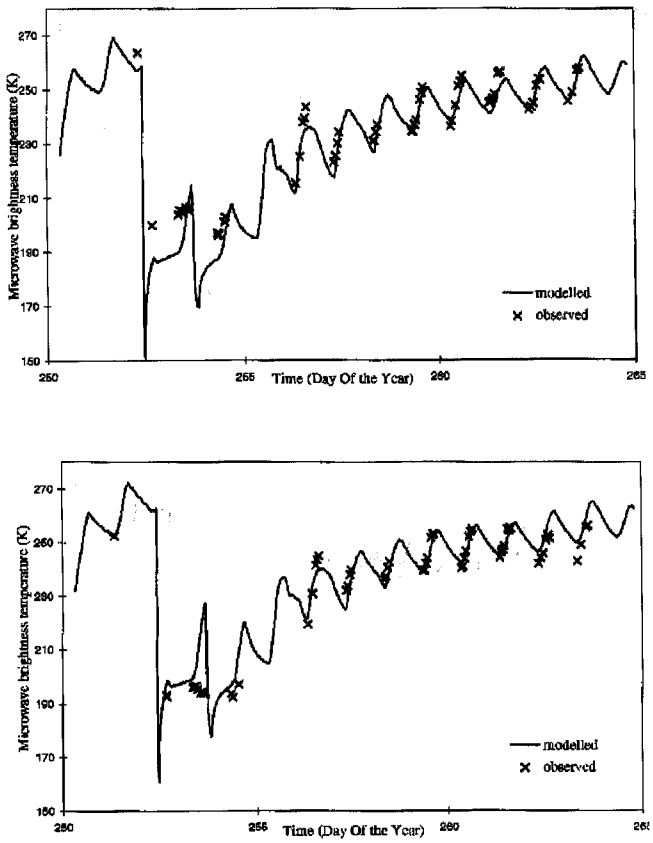

Fig. 1. *The time courses of the predicted (solid lines) and measured (points) microwave brightness temperature for (a) the loamy sand soil and (b) the loam, during the drydown following the 100 mm irrigation on day 252.*

The relation between microwave emission and near surface water content

A widely used approach to interpreting passive microwave radiometry is to establish an empirical relation between the emissivity (usually expressed in terms of a normalised brightness temperature) and some average near-surface soil water content (such as the average water content of the upper 2 or 5 cm of the soil profile) obtained by direct

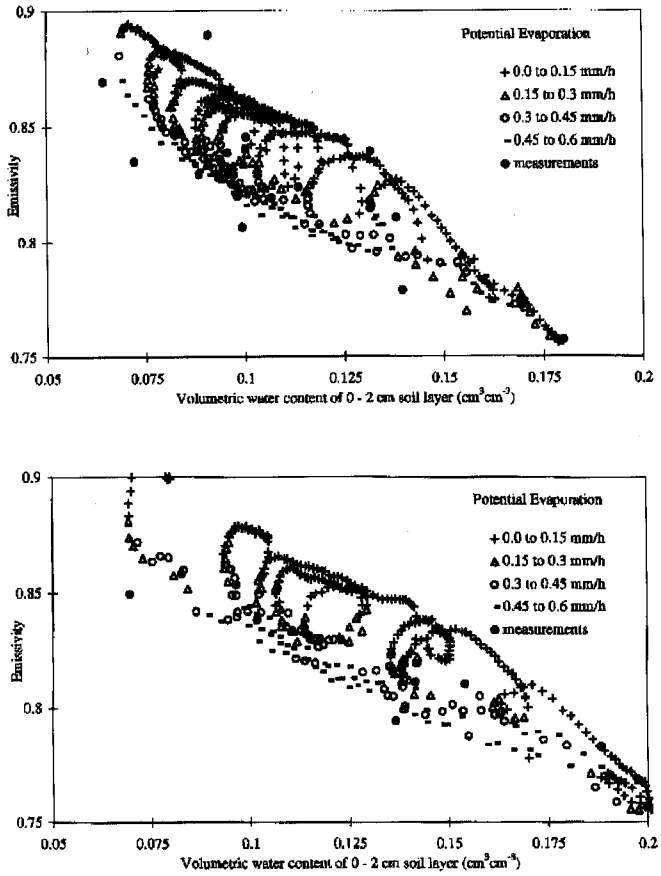

Fig. 2. *The simulated (small points) and measured (large points) relations between the microwave brightness temperature normalised with respect to the radiometric surface temperature and the average volumetric water content of the upper 2 cm of the profile for (a) the loamy sand and (b) the loam soil. The points derived from the simulation have been grouped into classes of evaporative demand.*

measurement. Such calibrations usually have considerable scatter (even when the analysis is restricted to smooth, unvegetated surfaces which avoid the confounding influence of roughness and the vegetation canopy on microwave emission). In many cases, much of this scatter can be attributed to spatial variation in soil wetness, particularly when the scale of the measurement of soil water content is several orders of magnitude smaller than the footprint of the radiometer. However a number of other causes of scatter are considered below.

Figure 2 shows the relation between normalised brightness temperature and the average water content of the upper 2 cm of the soil profile ($\theta_{0\text{-}2}$) obtained from direct measurements (solid circles) and from MICRO-SWEAT predictions (open symbols) during the drydown period shown in Fig. 1. The points in Fig. 2 derived from MICRO-SWEAT have been grouped into classes of potential evaporation rate.

Normalisation of T_B is necessary to take account of the direct effect of soil temperature on T_B. In a remote

sensing context such normalisation is usually done with respect to a radiometric surface temperature (T_{surf}) which might be inferred from thermal IR radiometry. In Fig. 2, the simulated points (open symbols) show the relation between the T_B/T_{surf} and θ_{0-2} that was derived from the half-hourly predictions of MICRO-SWEAT for the loamy sand (Fig. 2a) and the loam (Fig. 2b). Half-hourly values for the radiometric surface temperature were not available, so the simulated brightness temperatures have been normalised with respect to the simulated physical temperatures at 0.8 cm depth. These were in close agreement with the radiometric soil surface temperatures that were measured simultaneously with the microwave emissions.

The time sequence of data presented in Fig. 2 is as follows. The start of the drydown sequence is at the right hand side (wettest soil). Successive days of drying are seen as a series of anti-clockwise loops that are displaced leftwards gradually as the soil dries. The top of each diurnal loop occurred during the night when the evaporative demand was low, whereas the bottom of each loop is around the time of peak demand (i.e. midday).

The large symbols in Fig. 2 show the relation between T_B/T_{surf} and θ_{0-2} that was obtained from direct measurements of T_B, the radiometric surface temperature and the average water content of the upper 2 cm of the profile. The degree of scatter is slightly greater than for the simulated data, partly because of spatial variability effects arising because the near surface water content was measured at a scale between one and two orders of magnitude smaller than the footprint of the radiometer. However, most of the scatter observed in the empirically-determined relation can be explained by the series of anticlockwise diurnal hysteresis loops that are evident in the simulated data as the profile dried from day to day.

During periods of low evaporative demand (i.e. early morning and late evening), the value of T_B/T_{surf} was much higher at a given average near-surface water content than during the middle of the day when the evaporative demand was large. This effect tended to become more pronounced as the soil became drier. One explanation for the apparent diurnal hysteretic loops in the relation between T_B/T_{surf} and θ_{0-2} is that the surface temperature is inappropriate for normalising the brightness temperature because it is unrepresentative of the temperature of soil below the surface which will be contributing to the microwave radiation emergent at the soil surface. Discrepancies would be greatest at times when there are steep temperature gradients close to the surface, during times of high energy loading (i.e. around mid-day) and when the soils are relatively dry, and so have low thermal conductivity.

The inappropriateness of T_{surf} as a normalising variable is well known, and alternative approaches have been developed which make use of temperatures deeper in the soil (e.g. Choudhury and Schmugge, 1982; Chanzy *et al.*, 1997). Figure 3 shows the result of normalising T_B with

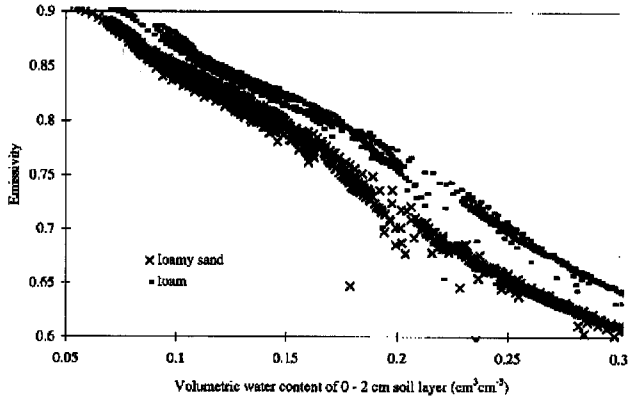

Fig. 3. *The relation between the microwave brightness temperature normalised with respect to the effective soil temperature (T_{eff}) and the average volumetric water content of the upper 2 cm of the soil profile. Note that a wider range of water content is covered than shown in Fig. 2.*

respect to the effective soil temperature (T_{eff}) derived from the Wilheit model embedded in MICRO-SWEAT; T_{eff} is calculated as the mean temperature of the profile weighted by the relative contributions of individual soil layers to the microwave emission at the soil surface. The use of T_{eff} as the normalising temperature has a stronger physical basis than the temperature at any specified depth, although it is not measurable directly. Time courses for the normalising temperatures used in Figs 2 and 3 are shown in Fig. 4. Also shown is the soil temperature at 10 cm depth, which was very close to the value of T_{eff}.

Normalising with respect to T_{eff} reduces the diurnal hysteresis substantially, T_{eff} has much less diurnal variation than the temperature at (or very close to) the soil surface. Figure 5 shows, for the loamy sand, the time course of the weighted average depth (z_t, Eqn. 4) of the source of the microwave radiation emergent at the soil surface which was derived from the Wilheit model. During the drydown

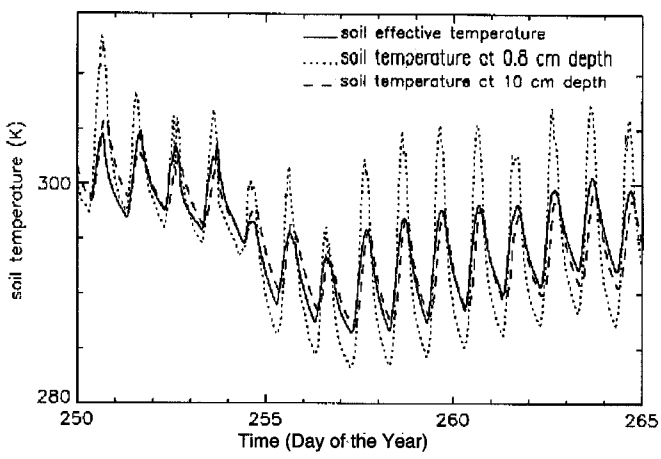

Fig. 4. *The time courses of soil temperature during the drydown period shown in Fig. 1.*

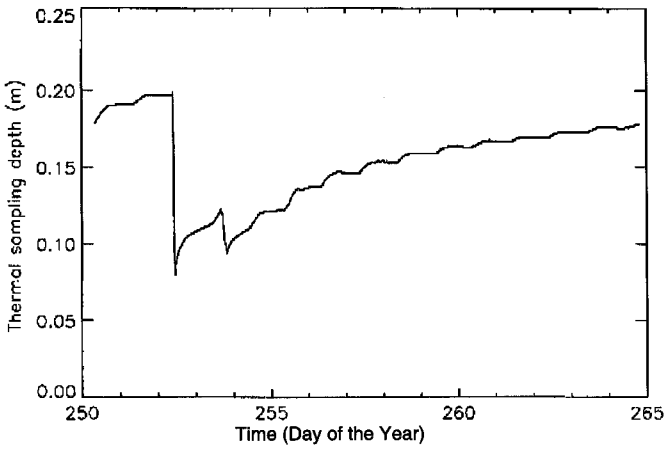

Fig. 5. *The time course of the weighted average soil depth contributing microwave emission that is emergent at the soil surface.*

period, z_t ranged from about 8 cm immediately after irrigation to about 18 cm after prolonged drying. This is consistent with T_{eff} being approximated reasonably by the temperature at 10 cm depth.

Steep gradients in water content, as well as in temperature, may also explain in part why there is an apparent diurnal variation in the relation between T_B/T_{surf} and θ_{0-2}. Figure 2 implies that soils exposed to a large evaporative demand appear to be wetter (i.e. have a lower normalised brightness temperature) than soils which have the same average water content in the 0–2 cm layer but are exposed to a low evaporative demand. Figure 6 compares the different profiles of the same average soil water content but different vertical distributions, during the drydown obtained at times with contrasting evaporative demand. A significant proportion of the microwave radiation emergent at the soil surface is emitted from depths greater than 2 cm (Fig. 5). If so, soil profiles subject to a large evaporative demand (i.e. with steep near-surface gradients in soil water

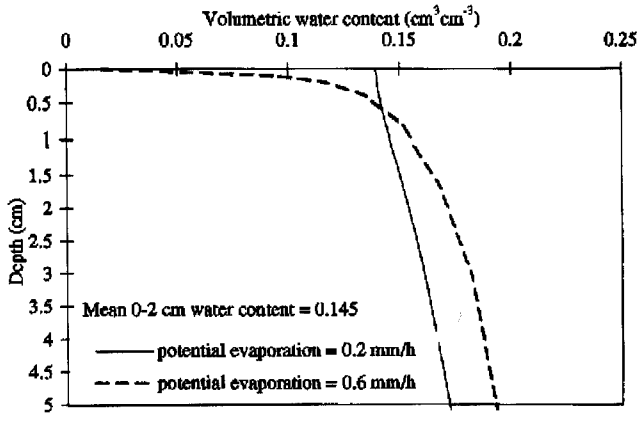

Fig. 6. *An example of the comparison between the profiles of soil water content obtained under conditions of high and low evaporative demand, and times when there was the same value for the average water content of the upper 2 cm of the profile.*

content and relatively wet soil below 2 cm) might be expected to have a lower apparent emissivity at a given value of θ_{0-2} than a soil profile with a more uniform distribution of water. However, the two evaporative demand situations in Fig. 6 had very similar values for T_B/T_{eff} (both were 0.79) implying that differences in the detailed shapes of the profiles in water content had remarkably little influence on the apparent emissivity.

There was a marked difference between the soils in the relation between the normalised brightness temperature and the average near-surface water content (Fig. 2) which remained evident when T_{eff} was used as the normalising temperature (Fig. 3). This influence of soil type has a number of strongly interacting causes that are difficult to distinguish. Soils with higher clay content will have a greater proportion of bound water, which will tend to reduce the soil dielectric at a given water content. This is consistent with the loam soil tending to have the higher emissivity. The difference between the soil types in Fig. 3 might also be attributable to consistent differences between the soils in the shapes of their temperature and water content profiles when the soils were compared at times when they had similar values for θ_{0-2} and were exposed to a similar atmospheric regime. This might imply systematic differences between the soils in the vertical distribution of the source of microwave radiation emergent at the soil surface. However, the earlier discussion of Fig. 6 illustrates that this does not necessarily imply there will be differences in the apparent emissivity of the soil surface. Whatever the cause of the differences between soils in the relation between near surface water content and apparent emissivity, these complex interactions have been accounted for successfully by MICRO-SWEAT; the simulated data have predicted the differences between soil types in the empirically-determined relation between T_B/T_{surf} and θ_{0-2} (closed circles, Figs. 2a and 2b).

The relation between soil surface resistance and near surface water content

Remote sensing of near-surface soil moisture is of use to hydrologists if it assists in the estimation of hydrological fluxes and evaporation from the soil surface, which is strongly dependent on the near surface water status. A widely used approach assumes that a dry soil surface acts as a diffusive resistance (r_s) interspersed between free water and the overlying air, in which case evaporation can be estimated using the Penman-Montieth equation with appropriate parameterisation of r_s. Analysis of the evaporation rates predicted by SWEAT through the drydown periods shown in Fig. 1, enabled the corresponding time courses of r_s to be estimated for the two soils as follows:

$$r_s = \left(\frac{e_{sat} - e}{E}\right) - r_a \qquad (5)$$

where e_{sat} is the saturated vapour concentration at the surface temperature, e is the vapour concentration at the

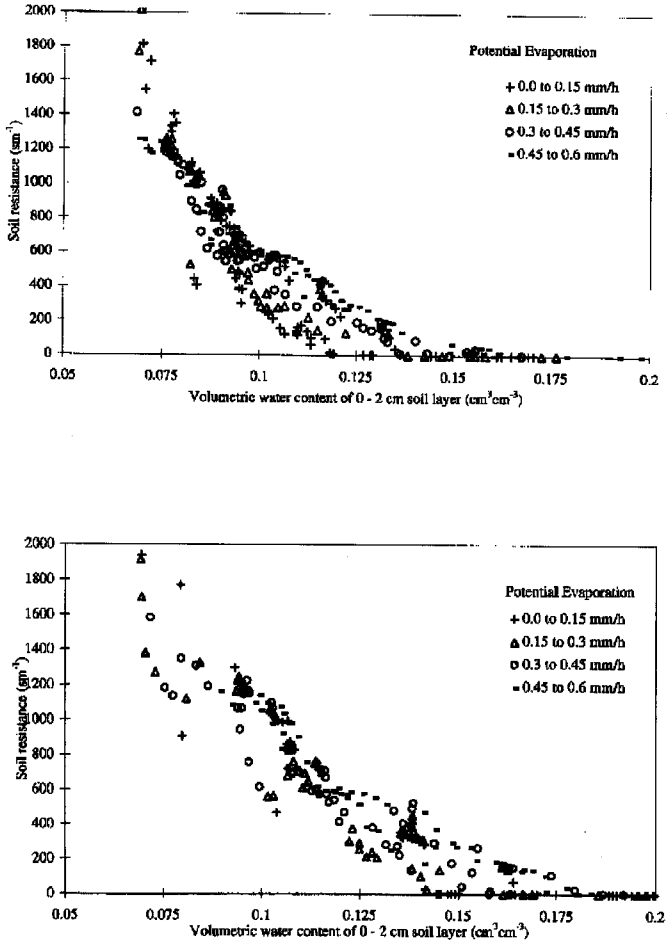

Fig. 7. *The relations between soil surface resistance and the average volumetric water content of the upper 2 cm of the profile for (a) the loamy sand and (b) the loam. The points have been subdivided into classes of potential evaporation rate.*

reference height, E is the evaporation rate direct from the soil surface and r_a is the aerodynamic resistance to vapour flow between the soil surface and the reference height.

Figure 7 shows, for the two soils, the relations established using MICROSWEAT between r_s and the average water content of the upper 2 cm of the soil profile. As in the case of the sandy soil studied by Daamen and Simmonds (1996), there was considerable scatter in the relation between r_s and $\theta_{0\text{–}2}$; this was attributable to variation in the evaporative demand. For a given average water content in the upper 2 cm, soils exposed to larger evaporative demand would have a steeper near-surface gradient in soil water content giving rise to a relatively large surface resistance. The relations between r_s and $\theta_{0\text{–}2}$ were very different for the two soils, as would be expected from the differences between the soils in their water retention and conductivity characteristics.

The original study of Daamen and Simmonds (1996) was prompted by the possibility of using microwave radiometry to sense, remotely, the average near-surface water content from which r_s might be inferred. However, it was shown earlier that the relation between $\theta_{0\text{–}2}$ and T_B/T_{surf} was not unique but, like r_s, had an apparent (albeit indirect) dependence on the prevailing evaporative demand, though this could largely be removed by normalising T_B with T_{eff}. The range of surface water content of interest with respect to r_s is at the dry end of the spectrum where steep gradients in near-surface water content are responsible for increasing surface resistance to vapour flow and, hence, is in the range greatest uncertainty in the relation between T_B/T_{surf} or T_B/T_{eff} and $\theta_{0\text{–}2}$. The apparent dependencies of T_B/T_{eff} and of r_s on the evaporative demand have the effect of partially offsetting one another if soil surface resistance is related directly to T_B/T_{eff}. Even so, plotting r_s directly against T_B/T_{eff} results in a relationship that still has considerable scatter; this can be largely accounted for by subdividing the data into classes of evaporative demand (Fig. 8). Table 1 shows for each of the soil types in Fig. 8, the regression equations relating r_s to T_B/T_{eff} within each band of potential evaporation rate.

Figure 9a compares the time course of evaporation predicted using SWEAT during the drydown period shown

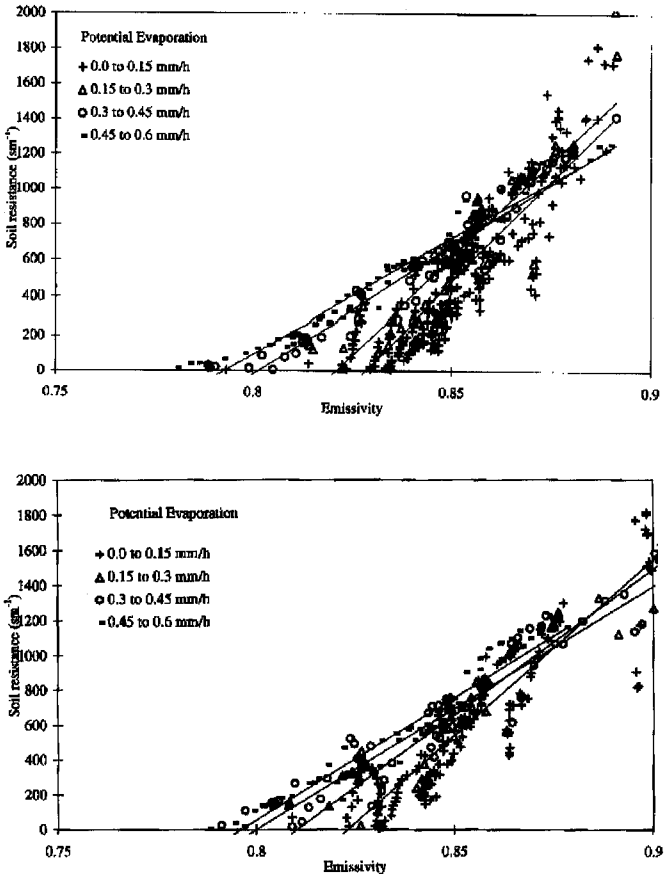

Fig. 8. *The relations between soil surface resistance and the microwave brightness temperature normalised with respect to the radiometric surface temperature for (a) the loamy sand and (b) the loam. The points have been subdivided into classes of potential evaporation rate.*

Table 1. The regression equations relating soil surface resistance (s m^{-1}) to the dimensionless microwave brightness temperature normalised with respect to the radiometric surface temperature.

	potential evaporation rate (mm h^{-1})	intercept (s m^{-1})	(s m^{-1})	r^2
Loamy sand	0.00–0.15	19677	−16158	0.74
	0.15–0.30	20138	−16253	0.89
	0.30–0.45	16921	−13425	0.90
	0.45–0.60	15561	−12176	0.91
Loam	0.00–0.15	20842	−16974	0.80
	0.15–0.30	19022	−15264	0.76
	0.30–0.45	15811	−12429	0.85
	0.45–0.60	17096	−13334	0.90

in Fig. 1 with that predicted using the Penman-Monteith equation with estimates of surface resistance derived from microwave brightness temperature using the regression equations in Table 1. Although the simulation in Fig. 9a was for the drydown period used to establish the relation between r_s and normalised brightness temperature (effectively ensuring good agreement between the two predictions of total evaporation), it is encouraging that the temporal patterns agree as well as they do. A better test is Fig. 9b, which shows the results of a similar exercise for the same soil, using the meteorological data for an earlier drydown period about 40 days previously during which the weather was rather different. Unfortunately, there were no independent measurements of evaporation from the soil surface to provide a more rigorous test of the prediction of evaporation. However, there is some confidence in the predictions of direct evaporation from the soil surface using SWEAT, which has been validated successfully against direct measurements using microlysimetry on sandy soils and sandy loam soils in Niger and India (Daamen and Simmonds, 1996) and, indeed, on the native sandy loam soil at the site of the experiment on which this paper is based (Burke, 1997).

Conclusions

The comparison of the simulations and measurements in Fig. 2 demonstrates that a physically-based model coupling microwave, energy and water flow can be used to establish the relationship between near-surface water content and brightness temperature based on *a priori* knowledge of the soil particle size distribution and the soil water retention and conductivity characteristics. The relation between near-surface water content and normalised brightness temperature can be influenced strongly by the prevailing atmospheric conditions and by soil type, both of which might be responsible in part for the scatter usually

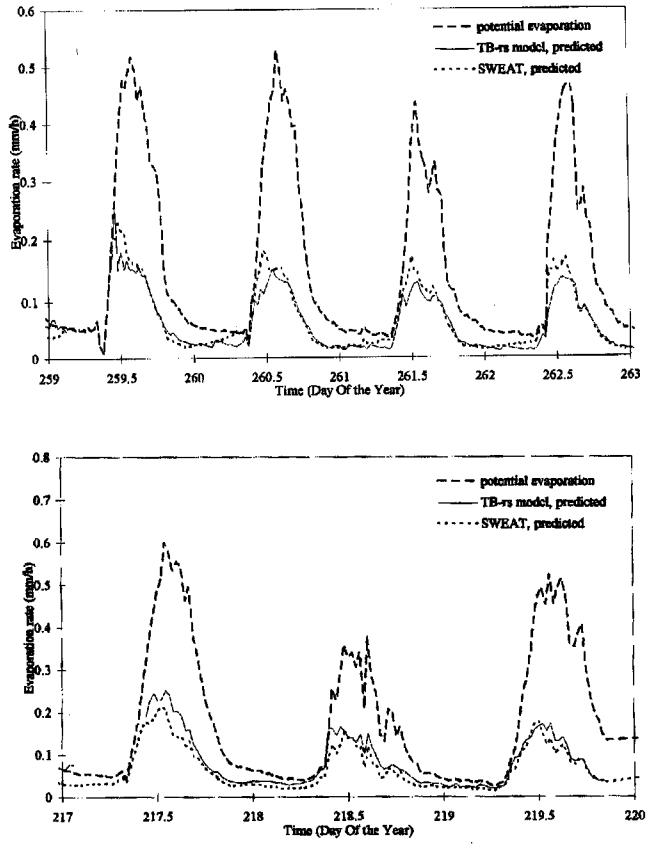

Fig. 9. *Comparison of the courses of evaporation for the loamy sand soil derived from brightness temperature (T_B) using the surface resistance/T_B relationship (Fig. 8) and predicted using SWEAT. (a) shows the period of the drydown used to derive Fig. 8, and (b) shows a different drydown period.*

observed in empirically-determined relations between T_B/T_{surf} and $\theta_{0\text{–}2}$. Much of this scatter may be attributed to T_{surf} being an inappropriate estimate of the effective soil temperature. For this reason, approaches have been developed (e.g. Choudhury and Schmugge, 1982; Chanzy *et al.*, 1997) in which estimates of T_{eff} (based on measured surface temperatures and temperatures deeper in the profile) are used to normalise T_B.

The present analysis was restricted to the case of a drydown following deep rewetting using 100 mm of irrigation. Shallow rewetting of a dry profile following a small rain event would likely give rise to a much higher normalised brightness temperature because of the contribution to the microwave signal from relatively dry soil below the wet near-surface; this could be an additional cause of scatter in empirically determined relations between T_B/T_{eff} and $\theta_{0\text{–}2}$. Furthermore, this analysis was restricted to smooth, bare soils, and so did not have the additional complications of surface roughness and a vegetation canopy to perturb the microwave emission.

These findings have a number of implications in a remote sensing context. Firstly, a number of the

complications in relating near surface water content to T_B arose because a significant contribution to the L band radiation emergent at the soil surface originated from below the near-surface layer being considered. While in this paper consideration was restricted to the water content of the upper 2 cm, similar (but less severe) complications arose in a corresponding analysis based on the water content of the upper 5 cm.

Secondly, the radiometric surface temperature is an inappropriate temperature to use for normalising T_B, though, in practice, this may often be the only temperature available in a remote sensing context. A pragmatic approach to improving the retrieval of near-surface water content from measurements of T_B/T_{surf} might be to take account of an additional measurable variable that is related (albeit indirectly) to the steepness of near-surface gradients in water content and temperature in order to explain some of the scatter in the relation between T_B/T_{surf} and $\theta_{0\text{–}2}$. Possible indicators which might be considered for this purpose include the downwelling or reflected solar radiation, which will be loosely correlated with the net radiation absorbed by the soil surface.

Thirdly, it has been shown that variability in soil texture is likely to confound the retrieval of near-surface water content from measured microwave brightness temperature. The effect of soil hydraulic properties on the relation between near-surface water content and T_B/T_{eff} is predictable using MICRO-SWEAT. The use of pedotransfer functions (which relate mapped soil texture units to soil hydraulic properties), coupled with models such as MICRO-SWEAT, might well improve the mapping of near surface water content using passive microwave remote sensing.

As well as being concerned with the retrieval of near-surface water content from measured microwave brightness temperature, this paper has explored the possibilities of making inferences about surface fluxes from L band radiometry. Using some average near surface water content as an intermediary in linking evaporation to remotely-sensed brightness temperature is likely to introduce a significant source of error that can be reduced by more direct relationships with surface resistance. Although this study was restricted to the relatively simple situation of the drydown of a smooth, bare soil following deep rewetting, the results illustrate the potential for making inferences about land surface processes using remote sensing in conjunction with physically based models of land surface/subsurface processes.

Acknowledgements

The authors acknowledge with gratitude the assistance of Peggy O'Neill (NASA Goddard Space Flight Center) in making available the data from the 1985 experiment. This project was carried out within a NERC TIGER programme project (project number GST/02/603). EJB was funded by a NERC studentship (GT4/93/24/P).

References

Bruckler, L. and Witono, H., 1989. Use of remotely sensed soil moisture content as boundary conditions in soil-atmosphere water transport modelling. 2. Estimating soil water balance. *Wat. Resour. Res.*, **25**, 2437–2447.

Burke, E.J., 1997. Using a modelling approach to predict soil hydraulic parameters from passive microwave measurements for both bare and cropped soils. PhD Thesis. University of Reading.

Burke, E.J., Gurney, R.J., Simmonds, L.P. and Jackson, T.J., 1997a. Calibrating a soil water and energy budget model with remotely sensed data to obtain quantitative information about the soil. *Wat. Resour. Res.*, **33**, 1689–1697.

Burke, E.J., Gurney, R., Simmonds, L.P. and O'Neill, P.E., 1997b. Using a modelling approach to predict soil hydraulic properties from passive microwave measurements. *IEEE Trans. Geosc. Remote Sens.* **36**, 454–462.

Camillo, P.J. and Gurney, R.J., 1986. A resistance parameter for bare-soil evaporation models. *Soil Sci.*, **104**, 95–105.

Chanzy, A., Bruckler, L. and Perrier, A., 1995. Soil evaporation monitoring—a possible synergism of microwave and infrared remote-sensing, *J. Hydrol.*, **165**, 235–259.

Chanzy, A., Raju, R.J. and Wigneron, J.P., 1997. Estimation of soil microwave effective temperature at L and C bands. *IEEE Trans. Geosc. Remote Sens.*, **35**, 570–580.

Choudhury, B.J. and Schmugge, T.J. 1982. A parameterisation of effective soil temperature for microwave emission. *J. Geophys. Res.*, **84**, 287–294.

Daamen, C.C. and Simmonds, L.P., 1996. Measurement of evaporation from bare soil and its estimation using surface-resistance. *Wat. Resour. Res.*, **32**, 1393–1402.

Jackson, T.J. and Schmugge, T.J., 1989. Passive microwave remote sensing system for soil moisture, some supporting research, *IEEE Trans. Geosc. Remote Sens.*, GE **27**, 225–235.

Mahfouf , J.F. and Noilhan, J., 1991. Comparative study of various formulations of evaporation from bare soil using in situ data. *J. Appl. Meteorol*, **30**, 1354–1365.

Schmugge, T.J., O'Neill, P.E. and Wang, J.R., 1986. Passive soil moisture research. *IEEE Trans. Geosc. Remote Sensing*, GE **24**, 12–22.

Schmugge, T.J. and Choudhury, B.J., 1981. A comparison of radiative transfer models for predicting the microwave emission from soils, *Radio Sci.*, **16**, 927–938.

Schmugge, T.J. and Jackson, T.J., 1994. Mapping surface soil moisture with microwave radiometers, *Meteorol. Atmos. Phys.*, **54**, 213–223.

Wang, J.R. and Schmugge, T.J., 1980. An empirical model for the complex dielectric permittivity of soils as a function of water content, *IEEE Trans. Geosc. Remote Sens.*, GE **18**, 288–295.

Wilheit, T.T., 1978. Radiative transfer in a plane stratified dielectric, *IEEE Trans. Geosc. Electronics*, **16**, 138–143.